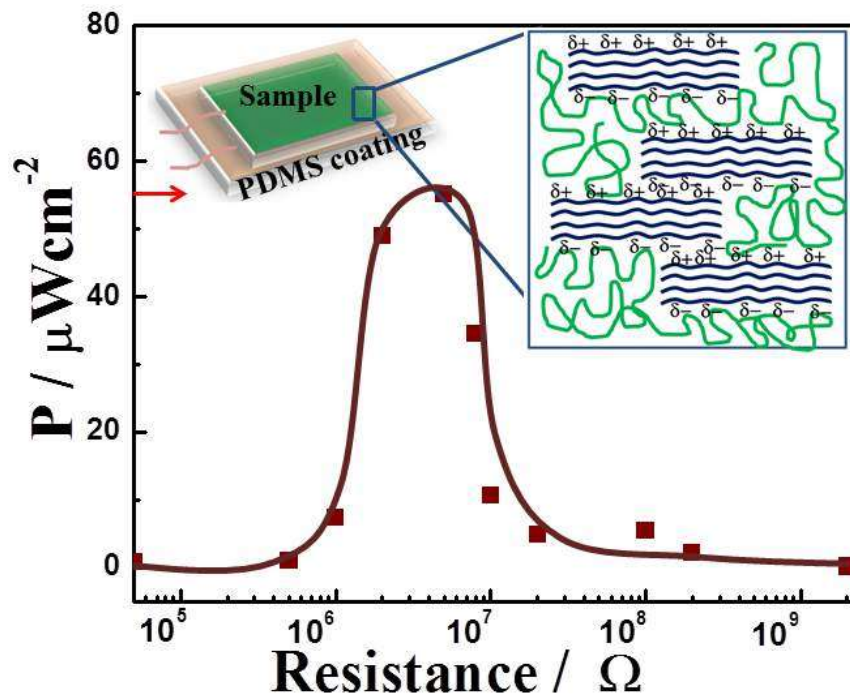


## Chapter 4

### Efficient Energy Harvesting Using Processed Poly(vinylidene fluoride) Nanogenerator



#### 4.1. Introduction:

Poly-(vinylidene fluoride) (PVDF) is a well-known piezoelectric polymer which has high flexibility, durability, high sensitivity to small mechanical forces, and high energy conversion efficiency, which are desirable properties for a good nanogenerator. PVDF have different phases ( $\alpha$ ,  $\beta$ ,  $\gamma$ ,  $\delta$ , and  $\epsilon$ ) obtained from different processing and nucleation methods [147]. Among these, polar  $\beta$  (TTTT) and  $\gamma$  ( $T_3GT_3\bar{G}$ ) phases are desirable as they exhibit high piezoelectric energy harvesting properties [148].  $\beta$ -phase is of more importance as it has better piezoelectric properties and large polarization sensitivity [149]. Different methods have been used to induce the electroactive  $\beta$ -phase in PVDF to obtain better piezoelectric properties, such as incorporation of 2-D nanomaterials like graphene [150-152], nanoclay [153, 154], and  $MoS_2$  [155]. Poling is done for stabilization of  $\beta$ -phase by alignment of  $-CH_2-/-CF_2-$  dipoles [46]. Addition of nanofillers without any electrical poling also enhances the polar electroactive phase [88, 90, 98]. Different researchers have fabricated energy harvesters with use of only PVDF or by adding a filler in it Bhavanasi et al. [156] prepared nanotubes of PVDF-TrFE through nanoconfinement and used them for energy harvesting under a dynamic compression pressure of 0.075 MPa which produces  $\sim 4.8$  V and  $2.2 \mu W/cm^2$  power. Laminated PVDF cantilever with magnetic mass for piezoelectric and electromagnetic energy harvesting produces 32 V and  $16 \mu W$  ( $4 \mu W/cm^2$ ) power at  $6 M\Omega$  resistance [85]. The maximum power of  $2 mW/cm^3$  is obtained for a cross-flow narrow stalk at wind speed of 2.8 m/s [86].

In the present work, an energy harvester using tough and processed PVDF at high temperature has been revealed without any filler incorporated in it. The enhancement of piezoelectric phase has been done through uniaxial stretching at elevated temperature, and a

device has been fabricated to generate power from waste mechanical energy. The reason for very high power generation has been revealed through the oriented structure of electroactive crystallites upon poling under high voltage demonstrating the potential of the developed polymeric material for nanogenerator suitable for miniature devices.

## 4.2. Experimental

Materials: SOLEF 6008 Poly(vinylidene fluoride), DMF, PDMS.

Thin film samples were prepared using compression molding machine. Samples of  $50 \times 15 \times 0.3$  mm<sup>3</sup> dimension were cut from the thin films for stretching purpose. Stretching of the sample is performed using universal testing machine at temperature of 90°C.

The details of PVDF sample abbreviations are as follows:

P: unstretched; P-S': half-stretched; P-S: fully stretched; P-S-5: stretched and poled at 500 kV/cm; P-S-10: Stretched and poled at 1000 kV/cm

## 4.3. Results and Discussion

### 4.3.1. Effect of Stretching on Structure and Properties

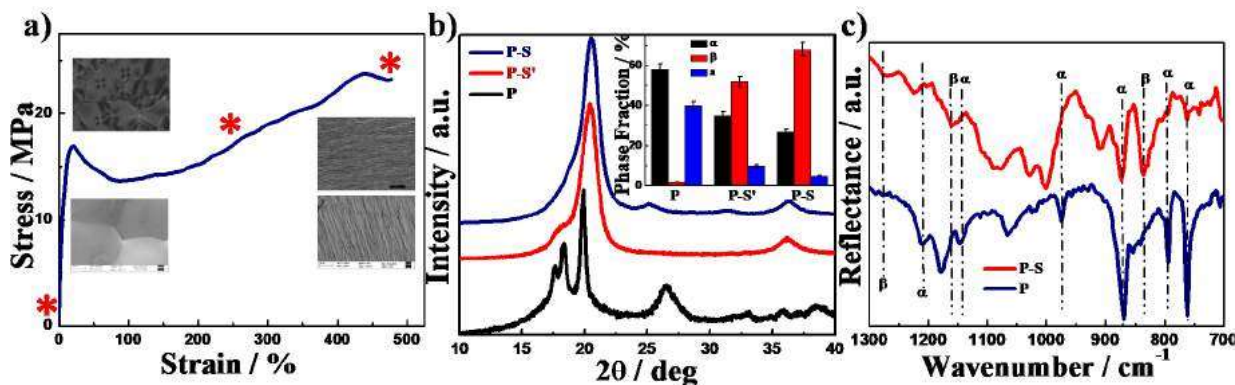


**Figure 4.1:** (a) Stress-strain curve of PVDF at elevated temperature (90 °C), polarized optical (lower images), and scanning electron microscopy images (top images) for corresponding marked (\*) positions (initial and final); (b) XRD patterns before stretching (P) and after stretching (P-S) showing intermediate pattern of taking sample (P-S') at middle asterisk marked position in stress-strain curve (inset diagram, phase fractions of different crystalline forms); and (c) FTIR patterns before and after stretching of the sample indicating absorption bands of various crystalline forms.

PVDF films are stretched uniaxially at elevated temperature to generate the piezoelectric phase in bulk, and the stress-strain curve obtained is shown in **Figure 4.1a**. The samples are stretched until the breaking point (nearly 500% elongation or draw ratio of ~5) to create a maximum electroactive phase. The changes in surface morphology at initial (before stretching) and at breaking points are shown both through scanning electron microscope and polarized optical microscope images (inset images of **Figure 4.1a**). A fine spherulitic pattern is evident before stretching which changes to fibrillar morphology after stretching as observed through optical images (inset lower micrographs of **Figure 4.1a**). Higher magnification images captured using SEM show tiny spherulite before stretching which converts into needle-like morphology after stretching indicating a possible change of structure (inset upper micrographs of **Figure 4.1a**) [141, 153, 157]. The structural alteration is confirmed through XRD analysis. Pristine PVDF (denoted as “P”) shows the peak positions at  $2\theta \sim 17.6^\circ(100)$ ,  $18.6^\circ(020)$ , and  $19.9^\circ(110)$  corresponding to  $\alpha$ -phase [139, 154], while the sole peak position for the stretched sample (draw ratio ~5) is shifted to higher angle at  $2\theta \sim 20.5^\circ(200/110)$  confirming the induced piezoelectric  $\beta$ -phase under uniaxial stretching (**Figure 4.1b**). This changeover of structure from  $\alpha \rightarrow \beta$  is further verified from the XRD pattern of sample (P-S') at lower draw ratio (~2.5, marked by middle \* in the stress-strain curve) which exhibits relatively weak peaks of the  $\alpha$ -phase and the dominant  $\beta$ -phase

demonstrating a gradual change of structure from non-piezoelectric TGT $\bar{G}$   $\alpha$ -phase to piezoelectric all-trans  $\beta$ -phase. At this juncture, it is important to know the relative amount of different crystalline phases as a function of draw ratio as calculated from the respective peak area after deconvolution of various peaks. It is interesting to mention that the content of  $\alpha$ -phase gradually decreases while the piezoelectric  $\beta$ -phase amount consistently increases with draw ratio and a maximum of 75% piezo-phase has been achieved at the draw ratio of  $\sim 5$  (inset image of **Figure 4.1b**). An upward trend after yielding phenomena, strain induced hardening, is due to crystallization, predominantly in the  $\beta$ -phase, which causes a systematic increase of the piezoelectric phase at the expense of the amorphous phase. This phase transformation is also verified through FTIR patterns for unstretched and stretched samples in **Figure 4.1c**. The peaks at 762, 794, 873, 974, 1142, and 1210  $\text{cm}^{-1}$  are assigned to  $\alpha$ -peaks before stretching while the peaks at 837, 1162, and 1278  $\text{cm}^{-1}$  are assigned to  $\beta$ -phase peaks only observed after stretching, indicating the evolution of the  $\beta$ -phase at the expense of the original  $\alpha$ -phase whose intensity diminishes significantly [140, 158]. However, the changeover of the structure from  $\alpha \rightarrow \beta$  is evident from both XRD and FTIR studies which also corroborates the alteration of morphology under uniaxial elongation.

#### 4.3.2. Energy Harvesting Using Direct Piezoelectric Effect

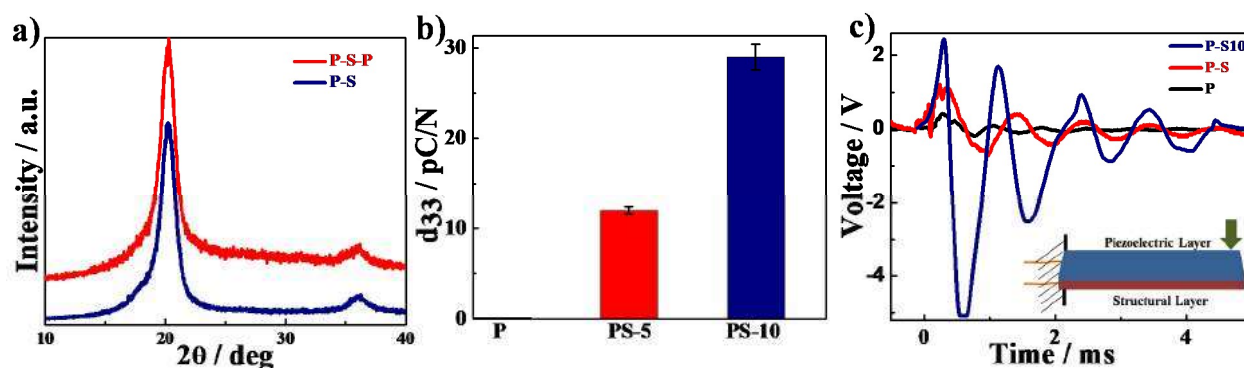


**Figure 4.2:** (a) X-ray diffraction pattern for unpoled and poled samples (b) Piezoelectric coefficient and (c) unimorph responses of stretched and poled samples.

The structural and morphological alteration clearly suggests greater piezoelectric content after the processing of PVDF films. This is to mention that the piezoelectric  $\beta$ -phase is having its dipole which is randomly oriented in the stretched film and needs to be oriented in a particular direction which in turn can increase the net charge separation. The samples are poled further to enhance the effective piezoelectricity in the sample. The poling process does not affect the structure; rather, it helps align the dipoles in the direction of applied field as evident from the XRD pattern shown in **Figure 4.2a**. The piezoelectric coefficients, a measure of piezoelectricity, exhibit very strong field dependency as evident from the higher  $d_{33}$  value of -30 pC/N against considerably the lower value of -12 pC/N at poling voltages of 10 and 5 kV/cm, respectively (**Figure 4.2b**). The poling process stabilizes the piezoelectric  $\beta$ -phase by aligning the dipoles [46]. However, the processed sample poled under higher potential exhibits very high piezoelectric coefficient even though the extent of piezoelectric phase is almost the same as evident from the deconvoluted XRD patterns of sample before and after poling. This is to mention that pure PVDF before stretching shows a negligibly small  $d_{33}$  value which after processing at high temperature under uniaxial stretching gives rise to a very high piezoelectric coefficient (-30 pC/N), and thereby it is expected to exhibit better energy harvesting through direct piezoelectric effect. The poled samples are used to make the unimorph as described in **Chapter 2**, and the voltage output is shown in **Figure 4.2c** as a function of time. The device using stretched PVDF shows moderately high voltage output ( $\sim 2$  V), while the same sample after poling at 10 kV/cm exhibits very high output voltage ( $\sim 7.5$  V) from the unimorph device prepared using structural and electroactive layers

(shown in the inset of **Figure 4.2c**). The impulse load is applied at one end of the cantilever, and voltage response is obtained from the samples. Pristine PVDF before processing shows meagre output voltage of  $\sim 0.7$  V, and more than one order higher magnitude is obtained from a processed and poled specimen indicating superior device activity.

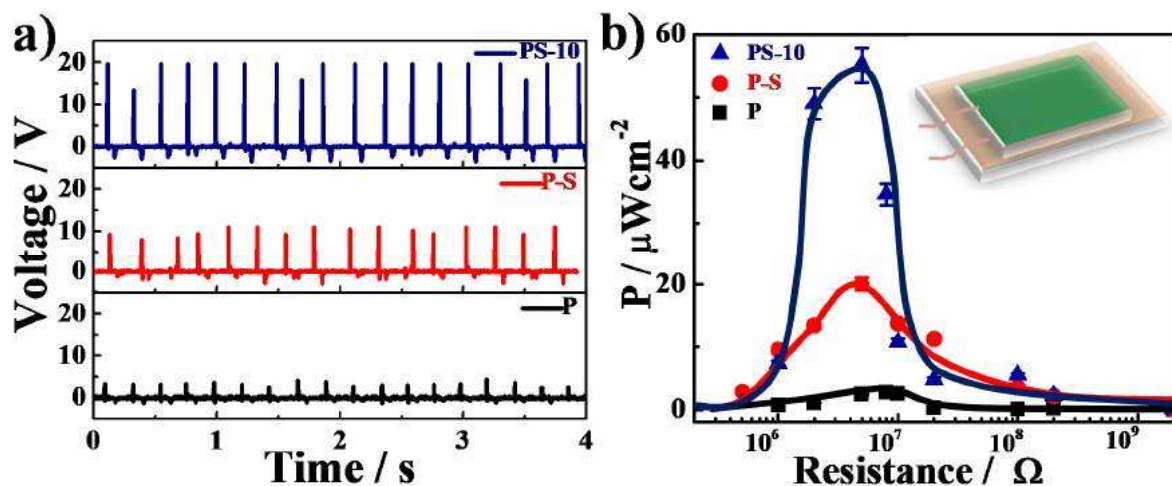


**Figure 4.3:** (a) open circuit voltage on finger pressing; (b) corresponding power of indicated unstretched, stretched, and poled samples.

Energy harvesting capability of the devices has been measured using different samples.

**Figure 4.3a** shows the open circuit voltage from the devices made of three different samples using the finger tapping method and a maximum peak to peak  $\sim 23$  V is obtained from the device using a processed and poled specimen (P-S-10) against the value of  $\sim 4$  V from an unstretched sample. Almost a systematic voltage output is obtained from consequent hitting from all of the devices with a value of  $\sim 12$  V output from the processed/stretched but unpoled sample. However, the processed and poled sample exhibits very high output voltage ( $\sim 20$  V), the schematic of device fabricated is shown in the inset of **Figure 4.3b**. The power is calculated from the output voltages from the finger pressing experiment at different

resistance using the relation  $P = V^2/R$ . The resistance at which maximum power is obtained is the optimum resistance for the material, and a very high power of  $55.2 \mu\text{W}/\text{cm}^2$  is achieved at an optimum resistance of  $5 \text{ M}\Omega$  (Figure 4.3b). The power obtained is the highest (more than one order higher) to date as per our knowledge.

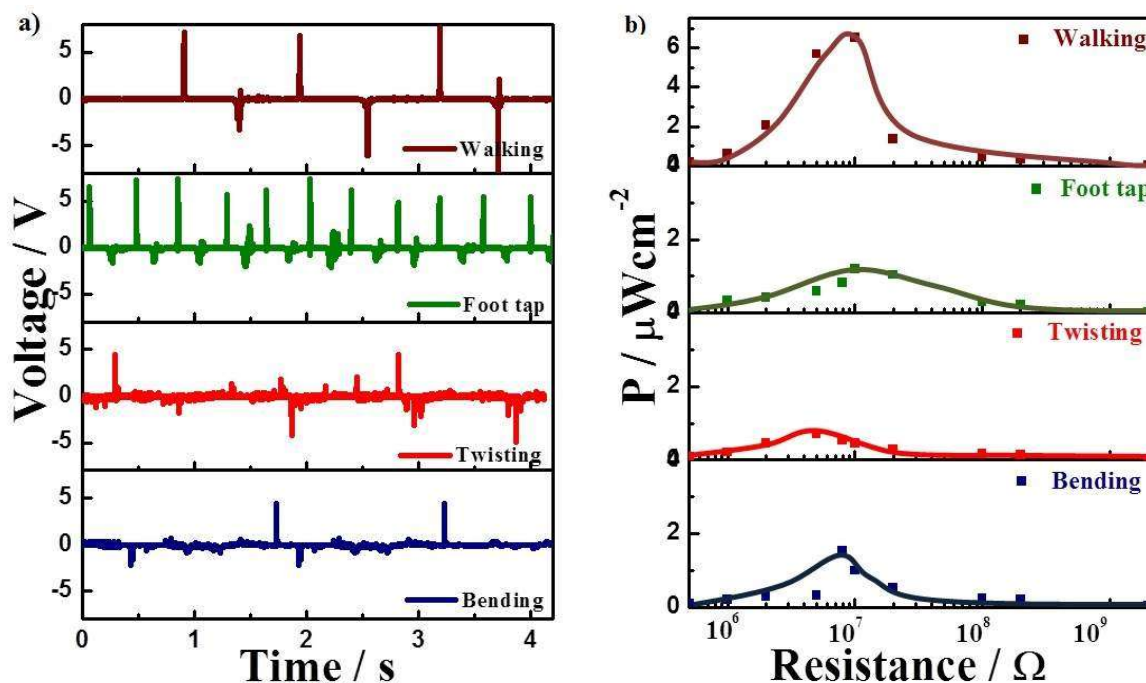


**Figure 4.4:** (a) open circuit voltage and (b) power density at different modes of application of stress like bending, twisting, foot tapping and walking.

Considering the thickness of electroactive material of  $\sim 100 \mu\text{m}$ , the power output becomes  $5.5 \text{ mW}/\text{cm}^3$ . This is worthy to mention that maximum 2.2 and  $4 \mu\text{W}/\text{cm}^2$  power outputs are reported using poled PVDF-TrFE nanotubes under a dynamic compression pressure and laminated PVDF cantilever with magnetic mass, respectively [85, 156]. However, this new and easy processing technique followed by poling with a suitably fabricated device exhibits very high power output of  $\sim 55 \mu\text{W}/\text{cm}^2$ . This device can also generate power from other



force loading modes such as twisting, foot tapping, bending, and walking and provide 0.7, 1.2, 1.5, and 6.5  $\mu\text{W}/\text{cm}^2$  power output, respectively. The details of open circuit voltages and power output at these modes are shown in **Figure 4.4a & b**. The power obtained from these modes is less than finger pressing, but they are sufficient to power the miniature devices as well and demonstrate the universality of the device made of simple but tough polymeric material with easy processability.

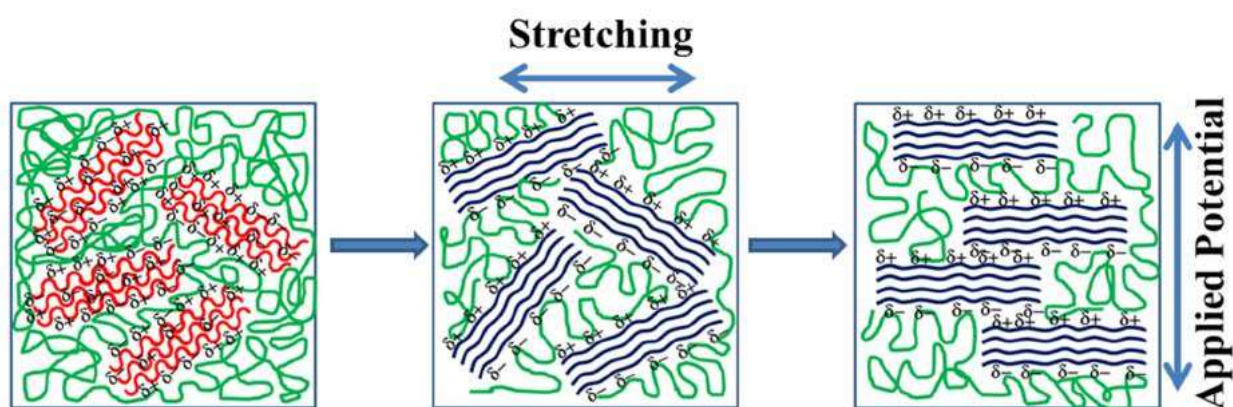


**Figure 4.5:** Schematic representation showing induction and orientation of piezoelectric phase in PVDF (red,  $\alpha$ -phase; blue,  $\beta$ -phase; green, amorphous phase).

It is very important to correlate the structural changes with uniaxial stretching. Higher elongation at break enhances the molecular chain alignment in the direction of stress, and this alignment helps PVDF chains to crystallize in all-trans planar zigzag conformation of  $\beta$ -phase [90, 154]. This is to mention that the  $\beta$ -phase (TTTT) is responsible for the electroactivity in PVDF. Further, orientation of the dipole gradually becomes perfect under poling condition which significantly improves the ultimate piezoelectricity even though the  $\beta$ -phase remains constant. The enhanced energy harvesting efficiency of the stretched and poled PVDF is due to change and orientation of electroactive phase in the polymer which is

explained in **Figure 4.5**. Pristine PVDF, having TGT $\bar{G}$  configuration, does not possess any net polarization in its molecule, while the all-trans (TTTT) configuration after stretching provides some amount of net polarization due to random orientation of the electroactive crystallites. On the other hand, well-oriented patterns of the electroactive crystallites generate maximum polarization in the specimen resulting in the highest piezoelectricity after poling the specimen at higher voltage. Further, greater toughness of the  $\beta$ -phase with its tiny mesh-like structure, as evident from SEM micrograph, makes the overall device robust for practical applications.

#### 4.3.3. Working Principle of charge generation in piezoelectric nanogenerator:

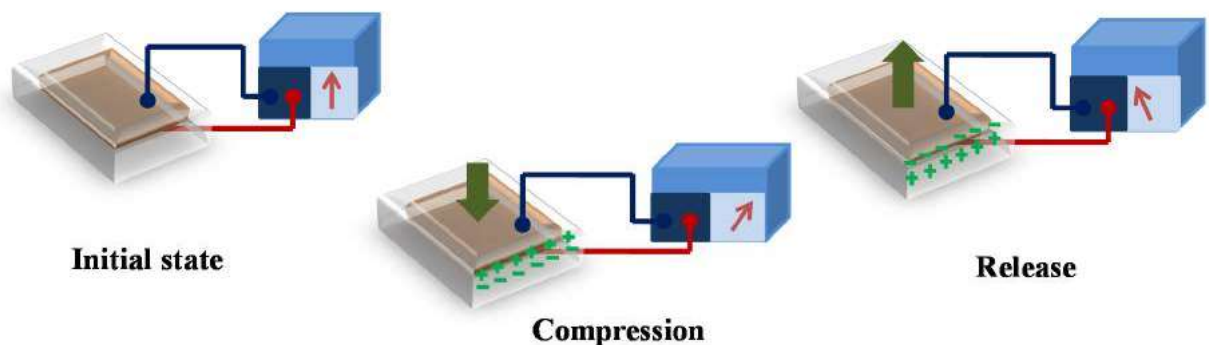


**Figure 4.6:** Working Principle of charge generation in device.

The working principle is shown in **figure 4.6**, in which there is no charge separation before applying stress, but with the application of external stress, there is generation of piezoelectric effect due to movement of dipoles in the lattice. The negative and positive surface charge is generated by the interaction between the generated dipoles [159, 160] and the dipoles are aligned perpendicular to the direction of applied mechanical stress by shear or stress induced

polarization. The negative and positive surface charge creates a potential difference between the electrodes and due to this potential difference there is flow of electrons from one electrode to the other. On the other hand, upon releasing the load or stress the piezoelectric potential disappears and the stored electrons flow in the opposite direction, which results in the signal in opposite direction [161].

#### **4.4. Conclusion**

An energy harvesting device with very high power output has been fabricated using conventional polymer such as PVDF. The electroactive/piezoelectric phase has been induced through uniaxial stretching of the rectangular samples at elevated temperature. The structural alteration is confirmed through X-ray diffraction and FTIR studies followed by the morphological changes typical for  $\beta$ -phase after high temperature processing. High piezoelectric  $\beta$ -phase content (~75%) exhibits a high piezoelectric coefficient of -30 pC/N upon poling at an electric field of 10 kV/cm. Unimorphs are made which show good output voltage as a function of time. An energy harvesting device has also been fabricated which exhibit high voltage output (23 V) with corresponding power density of 55.2  $\mu\text{W}/\text{cm}^2$  originating from finger pressing. The universality of power generation from various modes of force application have been tested and found suitable for energy generation for practical applications using easily processable and tough polymeric material from waste mechanical energy.